BOSTON UNIVERSITY

COLLEGE OF ENGINEERING

Dissertation

SPACE-TIME SAMPLING STRATEGIES FOR

ELECTRONICALLY STEERABLE INCOHERENT

SCATTER RADAR

by

JOHN SWOBODA

B.S., Rensselaer Polytechnic Institute, 2007

and

M.S.,Rensselaer Polytechnic Institute, 2008

Submitted in partial fulfillment of the

requirements for the degrees of

Doctor of Philosophy

2016

Approved by

First Reader

_____

Joshua Semeter, PhD
Professor of Electrical and Computer Engineering

Second Reader

_____

David Castanon, PhD
Professor of Electrical and Computer Engineering

Third Reader

_____

S. Hamid Nawab, PhD
Professor of Electrical and Computer Engineering

Forth Reader

_____

Philip Erickson, PhD
Atmospheric Sciences Group MIT Haystack Observatory

Ive learned that life is one crushing defeat after another until you just wish Flanders was dead.

Marge, this ticket doesn't just give me a seat. It also gives me the right, no, the duty to make a complete ass of myself.

The code of the schoolyard, Marge! The rules that teach a boy to be a man. Let's see. Don't tattle. Always make fun of those different from you. Never say anything, unless you're sure everyone feels exactly the same way you do.

To alcohol! The cause of, and solution to, all of life's problems.

Old people don't need companionship. They need to be isolated and studied so it can be determined what nutrients they have that might be extracted for our personal use.

Homer J. Simpson

Acknowledgments

Here go all your acknowledgments. You know, your advisor, funding agency, lab mates, etc., and of course your family.

As for me, I would like to thank Jonathan Polimeni for cleaning up old LaTeX style files and templates so that Engineering students would not have to suffer typesetting dissertations in MS Word. Also, I would like to thank IDS/ISS group (ECE) and CV/CNS lab graduates for their contributions and tweaks to this scheme over the years (after many frustrations when preparing their final document for BU library). In particular, I would like to thank Limor Martin who has helped with the transition to PDF-only dissertation format (no more printing hardcopies – hooray !!!)

The stylistic and aesthetic conventions implemented in this LaTeX thesis/dissertation format would not have been possible without the help from Brendan McDermot of Mugar library and Martha Wellman of CAS.

Finally, credit is due to Stephen Gildea for the MIT style file off which this current version is based, and Paolo Gaudiano for porting the MIT style to one compatible with BU requirements.

Janusz Konrad

Professor

ECE Department

SPACE-TIME SAMPLING STRATEGIES FOR ELECTRONICALLY STEERABLE INCOHERENT SCATTER RADAR

JOHN SWOBODA

Boston University, College of Engineering, 2016

Major Professor: Joshua L. Semeter, PhD
Department of Electrical and Computer Engineering,
Department of Astronomy

ABSTRACT

Have you ever wondered why this is called an *abstract*? Weird thing is that its legal to cite the abstract of a dissertation alone, apart from the rest of the manuscript.

.

Contents

ii

List of Tables

List of Figures

.

List of Abbreviations

ISR	. . . .	Incoherent Scatter Radar
IS	. . . .	Incoherent Scatter
AMISR	. . . .	Advance Modular Incoherent Scatter Radar
PFISR	. . . .	Poker Flat Incoherent Scatter Radar
RISR	. . . .	Resolute Bay Incoherent Scatter Radar
SuperDARN	. . . .	Super Dual Auroral Radar Network

Chapter 1

Introduction

Incoherent scatter radar (ISR), like all scientific instruments, is a testament to humankind's desire to understand the world around it. This even more so because they are generally very large and complicated systems that use substantial amounts of power, in the range of megawatts. These systems are able to probe Earths ionosphere and unlike other ground based measures this modality can give direct measurements of various plasma parameters including electron density (N_e), electron temperature (T_e), ion temperature (T_i) and ion velocity (V_i). ISRs has been in use since the 1950s (Gordon, 1958) and these systems have evolved over time from only being able to measure parameters along a single line of site to recently having the ability to be used as full 3-D sensors (Semeter et al., 2009), (Nicolls and Heinselman, 2007). The goal of this dissertation is to present a framework to analyze and improve the quality of the data that comes from modern ISR systems. This framework can help researchers improve their experiments and better understand the data products from ISR.

Until recently these systems were constructed using single, mechanically steered antennas. Because of this the rate that the look angle can change is limited by the mechanical speed of the *antenna pointing mechanism.* The newest generation of ISR **doesn't** systems are now taking advantage of electronically scanning phased array (ESPA), **sound** which allow for a near instantaneous change in the radar look direction. This thesis **right** will mainly focus on systems that are equipped with ESPA antennas, as they are the

impeddous for this work. Still many if not all of these ideas contained within can still be used by researchers using systems using single mechanically steered antennas or by individuals using the ESPA equipped ISR systems that using it to observe phenomena along just the range dimension.

1.1 Purpose

Some of the basics of ISR will be introduced in the following section. After which there will be a short discussion of the ionosphere and some of the phenomena that researchers use these systems to observe. Although the physics behind the ionosphere will not be discussed in detail, the section will help to elucidate some of properties of the system that will be studied. Following this will be a short introduction to some of the basic precepts behind inverse theory as used by engineers and scientists to analyze and improve the output of sensors.

1.1.1 Incoherent Scatter Radar

In order to produce plasma parameter measurements ISR systems radiate electromagnetic energy and monitor the reflected signal from free electrons in the ionosphere, or observe from other radiation sources in bistatic operation. This scatter has a specific spectral distribution which is driven by the values of the temperatures, densities and bulk flow of the plasma in the ionosphere. As such the two main steps in processing is the estimation of a power spectrum or autocorrelation function (ACF) and then fitting that to a physics based model at each point in time and space that the radar samples.

As stated previously ESPA antennas can create three dimensional reconstructions of plasma parameters. Examples of these new systems include The Advance Modular Incoherent Scatter Radars (AMISR), that have been developed and placed in Poker Flat Alaska and in Resolute Bay Canada (Semeter et al., 2009). These systems are

Figure 1·1: Image of the PFISR (SRI, 2016)

colloquially known in the research community as Poker Flat Incoherent Scatter Radar (PFISR), seen in Figure 1·1, and Resolute Bay Incoherent Scatter Radar (RISR). These systems have already started to give unprecedented views in the ionosphere and upper atmosphere and allowed for new types of measurements that were not possible before (Semeter et al., 2010) (Butler et al., 2010), (Nicolls and Heinselman, 2007). Currently EISCAT-3D is being developed as well and is expect do give even greater views due to the multi-static set up (eis, 2005).

1.1.2 Ionosphere and Phenomena

The ionosphere is the area of partially ionized gas, or plasma, surrounding the earth and in a way is like an interface between the earth and outer space (Kelly, 2009). The dynamics of this system are governed by kinetic, fluid and Maxwells equations coupled together (Schunk and Nagy, 2004). This complicated menagerie of equations allows for the creation of a cornucopia of different phenomena at any number of spatio-temporial scales.

When studying the ionosphere at times it helpful to look at a specific region. The high latitude ionosphere, which is the region close to the earth's magnetic poles, is of special interest due to the number of different phenomena that occur in this region.
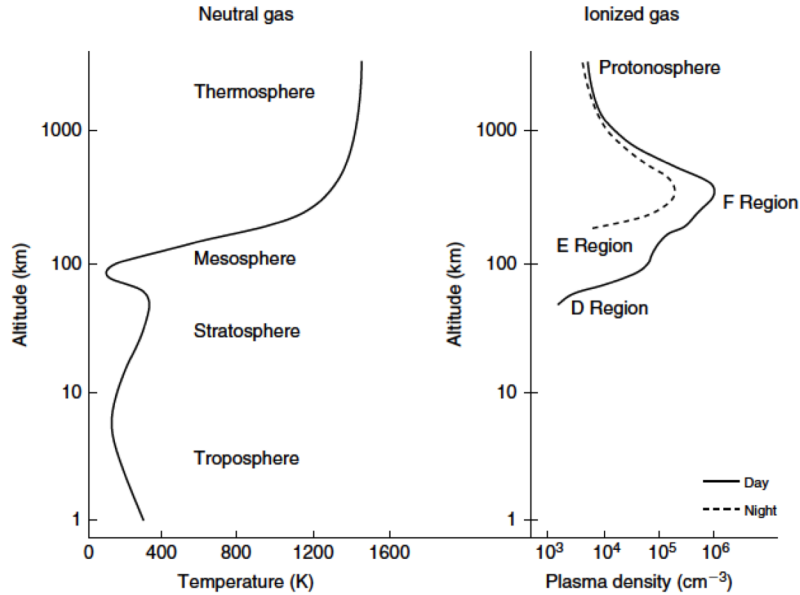
Figure 1·2: Example profiles of neutral temperature and plasma density from (Kelly, 2009)

These phenomena include but are not limited to aurora borealis, polar cap plasma patches and particle precipitation events.

The following is a listing of examples various types of high latitude ionosphere events grouped by specific behavior that is of interest the ISR sampling problem.

High Spatial Gradient Events

Polar cap patches are examples where of high spatial gradients in various plasma parameters (Dahlgren et al., 2012a),(Dahlgren et al., 2012b). In the polar cap large blobs of plasma with elevated electron density travel from the dayside to the night side ionosphere. These patches can play a large role in plasma transport within the polar ionosphere and interfere with radio transmission as well. Examples of sensor data that show these patches can be seen in Figure 1·3.

Large horizontal gradients also occur during geomagnetic storms which can produce large flows. This can create large disparities in Ion temperature as heating
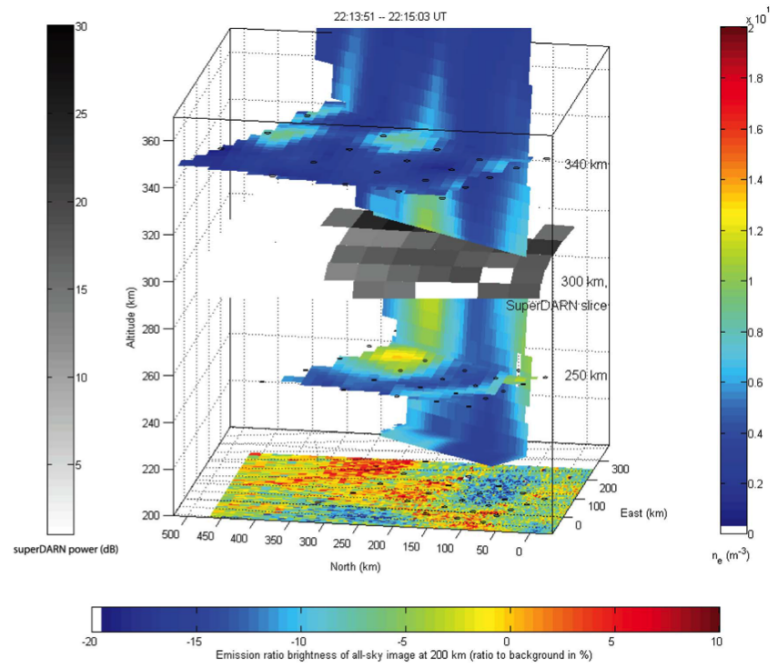
Figure 1·3: Example of polar cap patches seen in RISR and Super-DARN, from (Dahlgren et al., 2012a)

is occurring (Zettergren et al., 2008),(Zettergren and Semeter, 2012). During these storms ion temperatures can go from 500° K to over 1500° K in the order of kilometers.

These high gradient events can cause some upridictible errors where two plasma population interface. These errors can be quite complex due to the nonlinear nature of the inversion process(Vallinkoski and Lehtinen, 1990). Similar behavior has been observed during times of auroral turbulence where shear flows seems to have caused non isotropic temperature measurements(Knudsen et al., 1993).

High Speed Events

At times the ionosphere can be come locally unstable this can create a number of different types of turbulent events. Langmuir turbulence can create coherent structures that will be detected by ISR systems (Akbari et al., 2013). These structures change on the order of one pulse repetition interval of the radar.

1.1.3 Inverse Theory

Inverse theory gives engineers and scientists a robust frame work to determine the state of system parameters given a data set. Using the notation found in (Menke, 2012) a general inverse problem can be stated as follows,

$$\mathbf{d} = \mathbf{g}(\mathbf{m}) \tag{1.1}$$

where $\mathbf{d}$ is the data $\mathbf{g}$ is the operator that changes the parameters $\mathbf{m}$ to the data space.

Although Equation 1.1 gives a general framework this problem can be difficult to solve. Often, techniques used to solve inverse problems entail some assumption that can be made about the operator $\mathbf{g}$ such as linearity or that its well-posed. Still there are ways to get around this by doing things such as adding constraints or regularization to the inversion method.

ISR has in past been presented in this format, although this has mainly been for the case of a single beam. ISR can be thought of a general inverse problem because of the non-linear operation that brings the plasma parameters to the ACF space. Two schools of thought have emerged which in the community on how to be constrain these inversions. The first, full profile analysis uses plasma parameter constraints, which can give physical constraints to the inversion thus improving the outcome. The second set of techniques apply constraints on the estimated ACFs, which is less expensive computationally but can create ACFs that cannot be created through IS theory.

1.1.4 Outline of dissertation

Chapter 2 will go into the background into ISR signal processing. This will be begin by developing the basic signal model and carry through to show how complex voltages

become plasma parameter measurements. Chapter 3 will cover the Chapter 4 contains a discussion of the frame behind the Space-Time ISR Simulator (STISRS).

For this dissertation we will be proposing to improve the spatial and time sampling of the ISR systems. New phased array radar systems have allowed for an unprecedented amount of flexibility in sampling the environment. As such there has been no optimal way developed as of yet to sample this space. Currently ISR systems integrate their spectral estimate in time only. In order to get a statistical desirability of their measurements these systems may have to integrate for a long period of time. It may be possible to integrate across different beams if stationarity can be found. Other techniques could also be investigated such as well to try to improve the ISR measurements.

1.2   Contributions

Specific contributions of this research are summarized below.

1. Development of a theoretical framework for the forward model of 3-D ISR plasma parameter reconstructions.

2. Creating a framework full simulation of an ISR system that can which yield synthetic complex voltages.

3. A software package, named STISRS (Space-Time ISR Simulator), has be derived from previously mentioned simulation framework has been made available to other researchers.

4. A detailed analysis of the simulation framework using STISRS.

5. A new method for inverting the forward model 3-D ISR plasma parameter reconstructions.

Chapter 2

Incoherent Scatter Radar Processing

Radar is common remote sensing modality which has found diverse uses ranging from being used by police to monitor the speed of traffic (Richards et al., 2010), to mapping the surface of planets in our solar system (Campbell, 2002). The term radar itself is an acronym for radio detection and ranging, which the basic premise of these systems. These systems radiate electro-magnetic waves which reflect off of a target. These reflected waves are then received and processed by the system (Skolnik, 2008). The radar system measures the range R, or the distance between the target and sensor, by simply measuring the round trip time ΔT and using the following conversion,

$$R = \frac{c\Delta T}{2} \tag{2.1}$$

where c is the speed of light (Richards et al., 2010).

The main way to look at Doppler in hard-target radar is to assume it is a multiplication of the radar signal $s(t)$ with a simple single complex exponential

$$s_d(t) = s(t)e^{j\omega_d t}, \tag{2.2}$$

where ω_d is the Doppler frequency of the target or object. If we say have multiple targets each with their own Doppler frequency and their own weighting, which would represent a relative scattering to each components, we can represent that signal as the following

$$s_d(t) = \sum_n^N s(t)X(\omega_n)e^{j\omega_n t}. \tag{2.3}$$

Extending this to a continuum of signals each at each Doppler frequency this becomes

$$s_d(t) = \int s(t)X(\omega)e^{j\omega t}. \tag{2.4}$$

Pulling the $s(t)$ term out of the integral we can see that we are taking the Fourier transform of this relative weighting between each of the scatters and then multiplying it with the signal. Using simple Fourier properties we can see that this equivalent to a convolution in frequency space of the spectrum of the original radar signal and the Doppler spectrum with the collection of targets.

The final form of the signal spectrum with Doppler added can be shown as the following

$$s_d(t) = \int \left[\int S(\lambda)X(\lambda - \omega)d\lambda \right] e^{j\omega t}d\omega. \tag{2.5}$$

This shows that the measured Doppler on the radar signal can be formulated as the convolution of the Fourier transform of radar's signal along with the Doppler spectrum of the target.

Applying the Model To Pulse Doppler Radar

In pulse-Doppler (PD) radar a succession of pulses are sent out modulated by the carrier frequency f_c. Each pulse scatters off of the target and which imparts a Doppler frequency $\omega_d = 2\pi f_c \frac{2v}{c}$, where v is the target velocity and c is the speed of light. This representation of the Doppler frequency is only valid if the target is non-relativistic. In the case where we are looking at a single target the return of the mth pulse can be represented in the following way(Richards, 2005)

$$y(t) = A(t)e^{j\phi}e^{j\omega_d mT}, \tag{2.6}$$

where T is the pulse repetition interval (PRI). In this case each pulse is sampling the Doppler spectrum at a rate of the pulse repetition frequency (PRF). Using traditional PD processing the PRF determines the maximum unambiguous Doppler frequency. For example if one wants a system with a carrier frequency of 10 GHz that will resolve a target going the speed of sound with aliasing in Doppler (approximately 340 m/s) that system must have a PRF greater than 45 kHz if one uses the Nyquist theorem.

To get the final measurement of this spectrum often a Discrete Fourier transform is applied. When the data arrives to the radar it is sampled in to specific range gates and pulse samples. Pulse compression is applied across range to help to localize the signal in range. This operation is basically applying a filter that is the time reversed conjugate of the base band pulse. After pulse compression operation Discrete Fourier Transforms are taken across the pulse dimension in each range bin. The final result is commonly referred to as a range-Doppler map.

2.0.1 Applying the model to ISR

In some radar modalities the system is attempting to measure numerous targets. The number of targets grows the scatters resemble more of a distribution than a single scatterer. In the case of ISR the radar is trying to sample the velocity spectrum of the distribution of electrons in the upper atmosphere and ionosphere.

In ISR the goal of the system is often to sample what is called the ion-line spectrum. From Dougherty and Farley's 1960 paper (Dougherty and Farley, 1960) the normalized spectrum can be formulated as

$$X(\theta) = \frac{e^{-\theta^2}}{\pi\theta^2 e^{-2\theta^2} + (2 - I(\theta))^2}, \tag{2.7}$$

where $\theta = (\omega/k)\sqrt{m_i/(2KT_i)}$, K is Boltzman's Constant and $I(\theta)$ can be represented as the following:

$$I(\theta) = 2\theta e^{-\theta^2} \int_0^\theta e^{t^2} dt. \tag{2.8}$$

One can see in this formulation that the distribution is actually dependent on the thermal velocity of the ions $\sqrt{2KT_i/m_i}$. If one multiplies this velocity by the wavenumber k of the radar we actually get a Doppler frequency. This term is basically a normalization of the frequency space of the distribution to what would be the Doppler of the average thermal speed. The distribution $X(\theta)$ is basically the distribution of the scatterers at these different speeds.

To sample this spectrum one needs a process that can sample this frequency response. Although the function in Equation 2.7 has a number of assumptions built in one could still use it as a way to get a feel for what type of sampling frequencies are required. If we look at Figure **??** we can see it seems to have no appreciable content beyond $3\omega_\theta$, thus one needs a sensor that can sample at a frequency of at least $6\omega_\theta$ if we are using the Nyquist theorem. To give a rough example we can say that one wants to look at hydrogen ions at a temperature 600 Kelvin with a sensor that has a center frequency of 450 MHz [1]. This will yield an $\omega_\theta/2\pi$ of about 2 kHz and in order to sample that spectrum one would need to sample at about 12 kHz just to get this spectrum.

If one were to use a pulse-Doppler sort of approach to sampling the process used in the previous example one would need a PRF of about 12KHz. This PRF would only allow the pulse scatter off of a targets that are no more farther then 125km out. This would not work for ionosphere measurement when one want to measure out 700km.

In order to measure this spectrum ISR systems often use an intra-pulse autocor-

---

[1]This is a very simple example and probably not best for the ionosphere. I probably should use Oxygen ions or some other species for this example.

relation method to measure the Ion-line spectrum. To do this a pulse with a long time width is sent. The length is often on the order of a number of range bins. It is assumed that the plasma from different range's is uncorrelated but since the pulse is longer than a range bin energy scattered from other ranges are summed into other range bins. Once the correlations are formed a Fourier transform is taken of the autocorrelation functions (ACF), thus yielding a power spectrum for each range. This operation can also be described in terms of a Wigner-Ville distribution in that we are taking the Fourier transform of a time dependent correlation.[2] This spectrum is again the Doppler spectrum of the distribution of targets though and one is left with a range-Doppler map.

In a sense pulse-Doppler and ISR are attempting to measure the same quality, a Doppler spectrum of some target but they just have different measurement methods. In PD radar the Doppler spectrum is measured across the pulses while in ISR the Doppler spectrum is measured within the pulse itself.

This is mainly because of what the different systems are trying to measure. In most PD systems the required sample rate of the Doppler does not cause high enough PRFs to cause range ambiguities. Also in detection systems where point targets are being detected range (and Doppler) ambiguities can often be corrected.

In ISR the target being observed is a distribution of scatterers with a fairly large Doppler bandwidth. The large Doppler bandwidth along with the need to measure parameters at far ranges requires one to develop the Doppler spectrum using information that is available within a pulse. The pulses themselves are basically used as samples in an averaging of the autocorrelation function to develop a statistically significant representation of the spectrum.

---

[2]I need to work on the wording of this paragraph and add examples

2.1 Introduction

Incoherent scatter radar (ISR) is a powerful tool for exploring the ionosphere. These systems can give measurements of electron density N_e, ion temperature T_i, electron temperature T_e, ion velocity V_i and other plasma parameters (Dougherty and Farley, 1960; **?**; **?**; **?**). These parameters are measured by matching radar measured power spectra to a parameterized first-principles, physics based model of the power spectrum of the signal scattered from random ionospheric electron density fluctuations. Alternatively, fitting can be done in the lag domain by using the intrinsic autocorrelation function (ACF) of the plasma, which can be determined by taking an inverse Fourier transform of the power spectrum(Lehtinen and Huuskonen, 1996).

The spectral measurement process is fundamentally an estimation of a second order statistic of an inherently random process from the scattering of electrons. In order to get an estimate of the ACF with reasonable statistical properties, an ensemble average must be performed by averaging power spectra or autocorrelation functions together from different pulses. With traditional dish antennas, ISR systems build statistics in a limited number of ways. One method consists of pointing the radar beam in a specific direction and dwelling until enough pulses are integrated to get the desired statistics. Alternatively, the beam can be scanned through a field of view, collecting pulses while moving. These techniques use an implicit assumption about the uniformity of the plasma parameters within a volume defined by the pulse shape and solid angle beam properties while pulses are being integrated. This leads to an assumption of stationarity of the ACF within a temporal and spatial resolution cell of the radar.

In many cases, especially in the high latitude ionosphere, this stationarity assumption is not met. Phenomena such as polar cap patches can drift at greater than 1 km/s, and thus the residency time of a particular plasma parcel within a radar

beam may be much shorter than the integration time required to estimate an ACF (Dahlgren et al., 2012b). In the auroral zone, ionospheric variations produced by auroral particle precipitation occur on similarly short time scales compared to the integration period (Zettergren et al., 2008).

Recently, electronically steerable array (ESA) technology has started to be leveraged by the ISR community. The Advanced Modular Incoherent Scatter Radar (AMISR) systems have already been deployed both at the Poker Flat Alaska (PFISR) and Resolute Bay Canada (RISR) geospace facilities. The European led EISCAT-3D project is currently being developed using phased array technology as well and will be capable of multistatic processing. These new systems are already being used in a number of different ways including creating volumetric reconstructions of plasma parameters (Semeter et al., 2009; **?**; **?**; Dahlgren et al., 2012a). These reconstructions primarily consist of recasting ISR data into a Cartesian space through interpolation, after parameters have first been fit in a spherical coordinate system. Others have reconstructed full vector parameters using estimates of the ion velocity which can be determined using the Doppler shift of spectra (Butler et al., 2010; Nicolls et al., 2014).

These new ESA based systems differentiate themselves from dish antennas in a fundamental way. Instead of dwelling in a single beam or scanning along a prescribed direction, an ESA can move to a different beam position within its field of view on a rapid, pulse by pulse basis. An illustration of the differences between ESA and conventional radar systems with respect to statistical integration of radar pulses, focusing on time history of beam positions, starts with the desired grid of geographic parameter coverage in Figure **??**. Figure **??** shows a possible path for a dish based antenna to cover this measurement space through moves to different beam positions through time, represented on the z-axis as pulse repetition intervals (PRIs). The dish

sweeps through the field of view in a continuous scan. In contrast, an ESA system can instead move from position to position in discrete steps as seen in Figure **??**. We note as well that the phased array antenna is able to collect data from different beams during overlapping time periods, creating a lattice like pattern. This type of pulse-to-pulse beam position change is very difficult to accomplish with dish antenna systems having significant pointing inertia.

The rapid steering ability of ESA systems relative to space-time sampling yields a new flexibility, in post processing, to statistically combine information from different beams using knowledge of the plasma velocity field, where this information is obtained either from external sources or from the Doppler shift of the ionospheric echoes themselves. This can help to relax the assumption of stationarity for plasmas that are evolving or changing their shape on time scales longer than the integration time. If the plasma moves into a different beam, returns from the same plasma can be integrated together with proper bookkeeping. This is contrary to the situation with dish antennas where returns from multiple plasma populations with different parameter sets are unavoidably averaged together.

In order to take advantage of new ESA flexibilities, this work puts forth the idea of the space-time ambiguity function. This concept extends the range ambiguity to all three spatial dimensions along with time. The goal of this paper is to develop a new formalism for treating space-time ambiguity for electronically steerable ISRs, and in particular ISRs that are capable of sampling a given volume on a pulse-by-pulse basis. This paradigm can also be applied to other types of ISR system designs as well, but much of the utility of using this new formalism is more straightforwardly realized with ESA based systems. An outline of the paper's development is as follows. After developing the ambiguity formalism, we will develop specific cases of the impact of the three-dimensional ambiguity on moving plasma using conditions characteristic

of polar cap patches. A simulation of a polar cap patch using a full ISR simulator, which creates ISR data at the I/Q level, will be shown. Lastly we will briefly discuss strategies that could improve measurements from electronically steerable ISR systems.

2.2 Space-Time Ambiguity

The space-time ambiguity can be thought of as a kernel to a combined volume and time integration operator. In the derivations that follow, we show that this ambiguity can be represented as a kernel operator in a Fredholm integral equation:

$$\rho(\tau_s, \mathbf{r}_s, t_s) = \int L(\tau_s, \mathbf{r}_s, t_s, \tau, \mathbf{r}, t) R(\tau, \mathbf{r}, t) dV\, dt\, d\tau \qquad (2.9)$$

where, for ISR, $L(\tau_s, \mathbf{r}_s, t_s, \tau, \mathbf{r}, t)$ is a blurring kernel over time and space, and $R(\tau, \mathbf{r}, t)$ indicates the plasma medium's autocorrelation function at the lag τ, time t, and position $\mathbf{r}$.

By using this formulation, many parallels between ISR and classic camera blurring problems can be made. In cameras, blurring can take place when an object moves over a space covered by one pixel while the shutter is open and the CCD is collecting photons. A diagram of this can be seen in Figure **??**. The same holds for the ISR measurement problem, except that the pixels are no longer square or continuous in Cartesian space and instead are determined by the beam shape and pulse pattern. This is shown in the diagrams in Figure **??**.

2.2.1 Coordinate System Definitions

Before we derive the full space-time ambiguity function, $L(\tau_s, \mathbf{r}_s, t_s, \tau, \mathbf{r}, t)$, we will start with defining our coordinate system. Our three dimensional coordinate system is defined as $\mathbf{r} = [x, y, z]^T$. For this coordinate system, $\mathbf{r} = [0, 0, 0]^T$ at the location of the radar and thus $r = |\mathbf{r}|$, also known as the range variable. This allows for the

use of polar coordinates $\mathbf{r} = [r, \theta, \phi]^T$ where θ and ϕ are, respectively, the observer's elevation and azimuth angles.

The radar samples this space at a set of discrete points which will be referred to as $\mathbf{r}_s = [x_s, y_s, z_s]^T$ along with the discretized range expression $r_s = |\mathbf{r}_s|$. The sampled space consists of a number of points, composed of range gates within a beam multiplied by the number of beams. These points can also be referred in polar coordinates $\mathbf{r}_s = [r_s, \theta_s, \phi_s]^T$, where θ_s and ϕ_s are, respectively, the observationally sampled elevation and azimuth angles.

For notation purposes, we use two different sets of time commonly known in the hard-target radar literature as fast-time, n and slow-time, t (Richards, 2005). Fast-time is used to describe processes with correlation time less than one PRI. Slow-time will be used for processes that decorrelate in time on the order of, or longer than, the system's PRI. In order to form estimates of ACFs with desired statistical properties, it is assumed that the plasma parameters parameters will change on the order of many tens to hundreds of PRIs in their stationary reference frame (i.e. remain wide sense stationary for this time). Generally, for incoherent scatter applications in the E-region of the ionosphere ($\approx$100 km altitude) and above, the decorrelation time is less than a PRI for systems with a center frequency in the UHF band, and thus ACFs must be formed over fast-time.

The terms n and t represent continuous variables, while n_s and t_s will be the fast time and slow time parameters sampled by the radar. The sampling rate of n_s is set by the rate at which the system's A/D converters are run. The sampling of t_s can, at the highest rate, be the PRI. At its lowest rate, it can be sampled once in a non-coherent processing interval (NCPI), or equivalently in a period of time it takes the radar to average the desired number of pulses for each beam.

2.2.2 Derivation

The physical scattering mechanism underlying ISR produces measurable radar scatter from electron density fluctuations in the ionosphere, $n_e(\mathbf{r}, n)$, at a specific wavenumber $\mathbf{k}$. These fluctuations scatter radio waves which can be observed by the receiver system of the radar (Dougherty and Farley, 1960). The emitted radar signal at the transmitter has a pulse shape $s(n)$ modulated at a central frequency creating a scattering wave number $\mathbf{k}$. Using the Born approximation, the signal received at time n, $x(n)$, can be represented as the following

$$x(n) = h(n) * \int \exp\left[-j\mathbf{k} \cdot \mathbf{r}\right] s\left(n - \frac{2r}{c}\right) n_e(\mathbf{r}, n) d\mathbf{r}, \qquad (2.10)$$

where $h(n)$ is the receiver filter and the $*$ represents the convolution operator. In modern ISR systems, this signal $x(n)$ is then sampled at discrete points in fast-time which will be referred to as n_s. The convolution and sampling operation can be brought in the integral as the following,

$$x(n_s) = \int \exp\left[-j\mathbf{k} \cdot \mathbf{r}\right] s\left(n - \frac{2r}{c}\right) n_e(\mathbf{r}, n) h(n_s - n) d\mathbf{r} dn \qquad (2.11)$$

Once the signal has been received and sampled, the autocorrelation function is then estimated from the sampled signal $x(n_s)$. The full expression of the underlying autocorrelation of this signal is the following,

$$\langle x(n_s) x^*(n_s') \rangle = \int \exp\left[-j\mathbf{k} \cdot (\mathbf{r}' - \mathbf{r})\right] s\left(n - \frac{2r}{c}\right) s^*\left(n' - \frac{2r'}{c}\right)$$
$$h(n_s - n) h(n_s' - n') \langle n_e(\mathbf{r}, n) n_e^*(\mathbf{r}', n') \rangle d\mathbf{r} d\mathbf{r}' dn dn', \quad (2.12)$$

where r' is the magnitude of the vector $\mathbf{r}'$. By assuming stationarity of second order signal statistics along fast time, we can then substitute the lag variables $\tau \equiv n' - n$,

and $\tau_s \equiv n'_s - n_s$. With these substitutions, Equation 2.12 becomes

$$\langle x(n_s)x^*(n_s + \tau_s)\rangle = \int \exp\left[-j\mathbf{k} \cdot (\mathbf{r}' - \mathbf{r})\right] s\left(n - \frac{2r}{c}\right) s^*\left(n + \tau - \frac{2r'}{c}\right)$$

$$h(n_s - n)h(n_s + \tau_s - n - \tau)\langle n_e(\mathbf{r}, n)n_e^*(\mathbf{r}', n + \tau)\rangle d\mathbf{r}d\mathbf{r}'dnd\tau \quad (2.13)$$

We can make a simplifying assumption at this point that the space-time autocorrelation function of $n_e(\mathbf{r}, t)$, $\langle n_e(\mathbf{r}, n)n_e(\mathbf{r}', n + \tau)\rangle$, will go to zero as the magnitude of $\mathbf{y} \equiv \mathbf{r}' - \mathbf{r}$ increases beyond the debye length (Farley, 1969). Thus, the rate which the spatial autocorrelation goes to zero will be such that $\tau \gg \frac{2||\mathbf{y}||}{c}$, allowing us to set $r = r'$ inside the arguments of s and h. This allows Equation 2.13 to be rewritten as

$$\langle x(n_s)x^*(n_s + \tau)\rangle = \int s\left(n - \frac{2r}{c}\right) s^*\left(n + \tau - \frac{2r}{c}\right) h(n_s - n)h^*(n_s + \tau_s - n - \tau)$$

$$\left[\int \exp\left[-2j\mathbf{k} \cdot \mathbf{y}\right] \langle n_e(\mathbf{r}, n)n_e^*(\mathbf{y} + \mathbf{r}, n + \tau)\rangle d\mathbf{y}\right] drdnd\tau. \quad (2.14)$$

The inner integral is a spatial Fourier transform evaluated at the wave number of the radar $\mathbf{k}$. By again asserting stationarity along fast time, we can represent the true ACF as the following,

$$R(\tau, \mathbf{r}) = \langle |n_e(\mathbf{k}, r, \tau)|^2\rangle \equiv \int \exp\left[-2j\mathbf{k} \cdot \mathbf{y}\right] \langle n_e(\mathbf{r}, b)n_e^*(\mathbf{y} + \mathbf{r}, n + \tau)\rangle d\mathbf{y}. \quad (2.15)$$

Now Equation 2.14 becomes

$$\langle x(n_s)x^*(n_s + \tau_s)\rangle = \int \langle |n_e(\tau, \mathbf{k}, \mathbf{r})|^2\rangle \left[\int s(n - \frac{2r}{c})s^*(n + \tau - \frac{2r}{c})h(n_s - n)h^*(n_s + \tau_s - n - \tau)dn\right] c$$

$$(2.16)$$

If n_s is replaced with $2r_s/c$ we can introduce the range ambiguity function $W(\tau_s, r_s, \tau, r)$

by doing the following substitution,

$$W(\tau_s, r_s, \tau, r) = \int s(n - \frac{2r}{c}) s^*(n + \tau - \frac{2r}{c}) h(2r_s/c - n) h^*(2r_s/c + \tau_s - n - \tau) dn. \quad (2.17)$$

Assuming, for the moment, that $R(\tau, \mathbf{r})$ only varies across the range dimension r, we can now represent this in the form of a Fredholm integral equation

$$\langle x(2r_s/c) x^*(2r_s/c + \tau_s) \rangle = \int W(\tau_s, r_s, \tau, r) R(\tau, r) dr d\tau. \quad (2.18)$$

The range ambiguity function, $W(\tau_s, r_s, \tau, r)$, can be thought of as a smoothing operator along the range and lag dimensions of $R(\tau, r)$. This result is also derived in (Nikoukar et al., 2008), (Woodman, 1991) and (Hysell et al., 2008)

The spatial ambiguity across azimuth and elevation angles is determined by the antenna beam pattern. In phased array antennas, this beam pattern is ideally the array factor multiplied by the element pattern (Balanis, 2005). The array factor is determined by a number of things including the element spacing and the wave number of the radar, k. For example, by making idealized assumptions with no mutual coupling and that the array elements are simple cross dipole elements, AMISR systems will have the following antenna pattern for pointing angle (θ_s, ϕ_s):

$$F(\theta_s, \phi_s, \theta, \phi) = \frac{1}{2}(1 + \cos(\theta)^2) \left[\frac{1}{MN} (1 + \exp\left[j(\psi_y/2 + \psi_x) \right]) \frac{\sin((M/2)\psi_x)}{\sin(\psi_x)} \frac{\sin((N/2)\psi_x)}{\sin(\psi_x/2)} \right]^2,$$
$$(2.19)$$

where $\psi_x = -kd_x(\sin\theta\cos\phi - \sin\theta_s\cos\phi_s)$, $\psi_y = -kd_y(\sin\theta\sin\phi - \sin\theta_s\sin\phi_s)$ and M is the number of elements in the x direction of the array, and N is the number of elements in the y direction(see Appendix: **??** for derivation).

The spatial ambiguity is a separable function made up of the components of $W(\tau_s, \tau, r_s, r)$ and $F(\theta_s, \phi_s, \theta, \phi)$. These two functions can be combined by multiply-

ing the two, creating the spatial ambiguity function $K(\tau_s, \mathbf{r}_s, \tau, \mathbf{r})$. This yields an expression for a single statistical realization of the ACF of the incoherent scatter random process, which will be referred to as $\rho(\tau_s, \mathbf{r}_s)$:

$$\rho(\tau_s, \mathbf{r}_s) = \int F(\theta_s, \phi_s, \theta, \phi) W(\tau_s, r_s, \tau, r) R(\tau, \mathbf{r}) dV \, d\tau, \qquad (2.20)$$

$$= \int K(\tau_s, \mathbf{r}_s, \tau, \mathbf{r}) R(\tau, \mathbf{r}) dV \, d\tau. \qquad (2.21)$$

A rendering of an example of this full spatial ambiguity function for an uncoded long pulse, with antenna pattern from Equation 2.19 for four beams, can be seen in Figure ??.

As mentioned above, this one pulse ACF estimate represents a single sample of a random process. In order to create a usable estimate, multiple samples of this ACF need to be averaged together to reduce the variance to sufficient levels in order to fit the estimate to a theoretical ACF that is a direct function of plasma parameter values. To show the impact of this averaging in creating the estimate of the ACF, we will add slow-time dependence to the expression for the medium ACF, which now becomes $R(\tau, \mathbf{r}, t)$, and will also add another separable function $G(t_s, t)$ to the kernel. This function $G(t_s, t)$ can be thought of as a sampling and blurring kernel for the ACF if the plasma parameters change within an NCPI. Since the amount of time that the radar pulse is illuminating the plasma in a point of space is very short compared to the PRI, $G(t_s, t)$ can take the form of a summation of Dirac delta functions

$$G(t_s, t) = \sum_{j=0}^{J-1} \alpha_j \delta(t - t_s - jT_{REV}), \qquad (2.22)$$

where J counts the number of pulses used over a NCPI, T_{REV} is the amount of time it takes the radar to revisit the specific beam and α_j represent the weights that the radar

assigns to the pulses. For systems using pulse-to-pulse steering, one strategy revisits each beam sequentially, in this case making $T_{REV} = N_{beam}T_{PRI}$, where N_{beam} is the number of beams and T_{PRI} is the PRI time period. For the case where weights are set to $1/J$, this operation simply averages the pulses. With Equation 2.22 incorporated into the overall ambiguity we obtain the full integral equation,

$$\rho(\tau_s, \mathbf{r}_s, t_s) = \int L(\tau_s, \mathbf{r}_s, t_s, \tau, \mathbf{r}, t)R(\tau, \mathbf{r}, t)dV\,dt\,d\tau. \tag{2.23}$$

The final kernel, $L(\tau_s, \mathbf{r}_s, t_s, \tau, \mathbf{r}, t) = G(t_s, t)K(\tau_s, \mathbf{r}_s, \tau, \mathbf{r})$, encompasses the full space-time ambiguity.

2.2.3 Ambiguity after Frame Transformation

We will now focus on the impact of the motion of plasma as it is going through the field of view of the radar. We will assume that the radar is integrating over a length of time T beginning at t_s. The kernel L will be represented as a separable function K and G as in Equation 2.23. In this case, G will be a summation of Dirac delta functions with weights of $1/J$. This will change Equation 2.23 to the following:

$$\rho(\tau_s, \mathbf{r}_s, t_s) = \int K(\tau_s, \mathbf{r}_s, \tau, \mathbf{r}) \left[(1/J) \int\limits_{t_s}^{t_s+T} \sum_{j=0}^{J-1} \delta(t - t_s - jT_{REV})R(\tau, \mathbf{r}, t)dt \right] dV\,d\tau. \tag{2.24}$$

Of specific interest in this study are instances in the high latitude ionosphere where embedded plasma structures are moving due to electric field drivers applied by the magnetosphere. In this case, it will be assumed that the plasma is a rigid object and will not deform with respect to $\mathbf{r}$ over time period $[t_0, t_0+T]$ where $T = JT_{REV}$ is the time for one NCPI. Also, it will be assumed that the plasma parcel moves with a constant velocity $\mathbf{v}$. Thus $R(\tau, \mathbf{r}, t) \Rightarrow R(\tau, \mathbf{r}+\mathbf{v}t)$. The assumption of rigidity can in

some cases be valid over the time period of the NCPI, on the order of a few minutes, while the plasma moves through the field of view of the radar. For example, in the high latitude ionosphere, large scale features in structures such as patches decay on the order of hours (Tsunoda, 1988). This assumption is useful because it allows our framework to analyze impacts of these plasma variations on the parameter resolution of ISR systems. With these assumptions, Equation 2.24 becomes,

$$\rho(\tau_s, \mathbf{r}_s, t_s) = (1/J) \int \int_{t_s}^{t_s+T} \sum_{j=0}^{J-1} \delta(t - t_s - jT_{REV})K(\tau_s, \mathbf{r}_s, \tau, \mathbf{r})R(\tau, \mathbf{r} + \mathbf{v}t)dtdVd\tau$$

(2.25)

A change of variables to $\mathbf{r}' = \mathbf{r} + \mathbf{v}t$ acts as a Galilean transform and applies a warping to the kernel, changing the frame of reference. Since $R(\tau, \mathbf{r}')$ is no longer dependent on t, Equation 2.25 can be integrated in time and becomes:

$$\rho(\tau_s, \mathbf{r}_s, t_s) = (1/J) \int \left[\sum_{j=0}^{J-1} K(\tau_s, \mathbf{r}_s, \tau, \mathbf{r}' - \mathbf{v}(t_s + jT_{REV})) \right] R(\tau, \mathbf{r}')dVd\tau. \quad (2.26)$$

The problem can now be simplified further back to a Fredholm integral equation by simply replacing the terms in the square brackets as a new kernel $A(\tau_s, \mathbf{r}_s, t_s, \tau, \mathbf{r}')$:

$$\rho(\tau_s, \mathbf{r}_s, t_s) = \int A(\tau_s, \mathbf{r}_s, t_s, \tau, \mathbf{r}')R(\tau, \mathbf{r}')dVd\tau. \quad (2.27)$$

The impact of the plasma velocity on the ambiguity function can be seen in Figure **??**. This is the same ambiguity as seen in Figure **??** but with a velocity of 500 m/s in the y direction over a period of 2 minutes. This velocity creates a larger ambiguity function in the frame of reference of the moving plasma.

The operator A can be determined through knowledge of the radar system's beam pattern along with the experiment's pulse pattern, integration time and inherent

velocity of the plasma. This velocity $\mathbf{v}$ could be separately estimated by taking measurements of the Doppler shift by using a methodology like that seen in (Butler et al., 2010). With this strategy, the operator is now acting purely as a spatial blurring function instead of a full space-time function. We note that reducing dimensionality of the problem can make it easier to solve the inverse problem in practice.

Chapter 3

Conclusions

3.1   Summary of the thesis

Time to get philosophical and wordy.

IMPORTANT: In the references at the end of thesis, all journal names must be spelled out in full, except for standard abbreviations like IEEE, ACM, SPIE, INFOCOM, ...

Appendix A

Proof of xyz

This is the appendix.

References

(2005). Eiscat 3d design specification document.

(2016).

Akbari, H., Semeter, J. L., Nicolls, M. J., Broughton, M., and LaBelle, J. W. (2013). Localization of auroral langmuir turbulence in thin layers. *Journal of Geophysical Research: Space Physics*, 118(6):3576–3583.

Balanis, C. A. (2005). *Antenna Theory: Analysis and Design*. Wiley-Interscience.

Butler, T. W., Semeter, J., Heinselman, C. J., and Nicolls, M. J. (2010). Imaging f region drifts using monostatic phased-array incoherent scatter radar. *Radio Sci.*, 45(5):RS5013.

Campbell, B. (2002). *Radar Remote Sensing of Planetary Surfaces*. Cambridge University Press.

Dahlgren, H., Perry, G. W., Semeter, J. L., St. Maurice, J. P., Hosokawa, K., Nicolls, M. J., Greffen, M., Shiokawa, K., and Heinselman, C. (2012a). Space-time variability of polar cap patches: Direct evidence for internal plasma structuring. *Journal of Geophysical Research: Space Physics*, 117(A9).

Dahlgren, H., Semeter, J. L., Hosokawa, K., Nicolls, M. J., Butler, T. W., Johnsen, M. G., Shiokawa, K., and Heinselman, C. (2012b). Direct three-dimensional imaging of polar ionospheric structures with the resolute bay incoherent scatter radar. *Geophysical Research Letters*, 39(5).

Dougherty, J. P. and Farley, D. T. (1960). A theory of incoherent scattering of radio waves by a plasma. *Proceedings of the Royal Society of London. Series A, Mathematical and Physical Sciences*, 259(1296):pp. 79–99.

Farley, D. T. (1969). Incoherent scatter correlation function measurements. *Radio Sci.*, 4(10):935–953.

Gordon, W. (1958). Incoherent scattering of radio waves by free electrons with applications to space exploration by radar. *Proceedings of the IRE*, 46(11):1824–1829.

Hysell, D. L., Rodrigues, F. S., Chau, J. L., and Huba, J. D. (2008). Full profile incoherent scatter analysis at jicamarca. *Annales Geophysicae*, 26(1):59–75.

Kelly, M. C. (2009). *The Earth's Ionosphere Plasma Physics and Electrodynamics.* Elsevier, second edition.

Knudsen, D. J., Haerendel, G., Buchert, S., Kelley, M. C., Steen, Å., and Brändström, U. (1993). Incoherent scatter radar spectrum distortions from intense auroral turbulence. *Journal of Geophysical Research: Space Physics*, 98(A6):9459–9471.

Lehtinen, M. S. and Huuskonen, A. (1996). General incoherent scatter analysis and {GUISDAP}. *Journal of Atmospheric and Terrestrial Physics*, 58(1–4):435 – 452.

Menke, W. (2012). *Geophysical Data Analysis: Discrete Inverse Theory: MATLAB Edition.* International Geophysics. Elsevier Science.

Nicolls, M. J., Cosgrove, R., and Bahcivan, H. (2014). Estimating the vector electric field using monostatic, multibeam incoherent scatter radar measurements. *Radio Science*, 49(11):1124–1139.

Nicolls, M. J. and Heinselman, C. J. (2007). Three-dimensional measurements of traveling ionospheric disturbances with the Poker Flat Incoherent Scatter Radar. *Geophysical Research Letters*.

Nikoukar, R., Kamalabadi, F., Kudeki, E., and Sulzer, M. (2008). An efficient near-optimal approach to incoherent scatter radar parameter estimation. *Radio Science*, 43(5).

Richards, M., Scheer, J., Scheer, J., and Holm, W. (2010). *Principles of modern radar.* Number v. 1 in Principles of Modern Radar. SciTech Publishing, Incorporated.

Richards, M. A. (2005). *Fundamentals of Radar Signal Processing.* McGraw-Hill.

Schunk, R. and Nagy, A. (2004). *Ionospheres: Physics, Plasma Physics, and Chemistry.* Cambridge Atmospheric and Space Science Series. Cambridge University Press.

Semeter, J., Butler, T., Heinselman, C., Nicolls, M., Kelly, J., and Hampton, D. (2009). Volumetric imaging of the auroral ionosphere: Initial results from pfisr. *Journal of Atmospheric and Solar-Terrestrial Physics*, 71:738 – 743.

Semeter, J., Butler, T. W., Zettergren, M., Heinselman, C. J., and Nicolls, M. J. (2010). Composite imaging of auroral forms and convective flows during a substorm cycle. *Journal of Geophysical Research: Space Physics*, 115(A8):n/a–n/a.

Skolnik, M. (2008). *Radar Handbook*. Electronics electrical engineering. McGraw-Hill.

Tsunoda, R. T. (1988). High-latitude F region irregularities: A review and synthesis. *Reviews of Geophysics*.

Vallinkoski, M. and Lehtinen, M. (1990). Parameter mixing errors within a measuring volume with applications to incoherent scatter. *Journal of Atmospheric and Terrestrial Physics*, 52(6–8):665 – 674. ¡ce:title¿The Fourth International {EISCAT} Workshop¡/ce:title¿.

Woodman, R. F. (1991). A general statistical instrument theory of atmospheric and ionospheric radars. *Journal of Geophysical Research*, 96(A5):7911–18.

Zettergren, M. and Semeter, J. (2012). Ionospheric plasma transport and loss in auroral downward current regions. *J. Geophys. Res.*, 117(A6):A06306.

Zettergren, M., Semeter, J., Blelly, P.-L., Sivjee, G., Azeem, I., Mende, S., Gleisner, H., Diaz, M., and Witasse, O. (2008). Optical estimation of auroral ion upflow: 2. a case study. *Journal of Geophysical Research: Space Physics*, 113(A7):n/a–n/a.

CURRICULUM VITAE

Joe Graduate

Basically, this needs to be worked out by each individual, however the same format, margins, typeface, and type size must be used as in the rest of the dissertation.